



J. Serb. Chem. Soc. 75 (3) 385–394 (2010)
JSCS–3971

Journal of
the Serbian
Chemical Society

JSCS@tmf.bg.ac.rs • www.shd.org.rs/JSCS

UDC 666.3–127.001:539.24:544.773.42/43

Original scientific paper

Preparation and morphology of porous SiO₂ ceramics derived from fir flour templates

ZHONG LI^{1,2}, TIEJUN SHI^{1*} and LIYING GUO¹

¹School of Chemical Engineering, Hefei University of Technology, Hefei 230009 and ²School of Chemical Engineering, Anhui University of Science & Technology, Huainan 232001, China

(Received 10 April, revised 25 November 2009)

Abstract: The preparation of SiO₂ ceramics with controllable porous structure from fir flour templates via sol–gel processing was investigated. The specific size of the fir flour, which was treated with 20 % NaOH solution, was infiltrated with a low viscous silica sol and subsequently calcined in air, which resulted in the formation of highly porous SiO₂ ceramics. X-Ray diffraction (XRD), Fourier transform infrared spectroscopy (FTIR) and field emission scanning electron microscopy (FESEM) were employed to investigate the microstructure and phase formation during processing as well as of the SiO₂ ceramics. N₂ adsorption measurements were used to analyze the pore size distributions (PSD) of the final ceramics. The results indicated that the surface topography was changed and the proportion of the amorphous material was increased in NaOH-treated fir flour. The final oxide products retained ordered structures of the pores and showed unique pore sizes and distributions with hierarchy on the nanoscale derived from the fir flour.

Keywords: porous silicon ceramics; microstructure; sol–gel process; calcination.

INTRODUCTION

Over the last decade, oxide ceramics with special structure and morphology have aroused widespread interest, one of which is SiO₂ with unique porous structures.^{1–5} Porous silicas have attracted considerable attention because of their distinguished performance in adsorption technology, catalysis, and medical applications. In general, biotemplating techniques, in which biological materials are used directly as template structures for high-temperature conversion into technical ceramic materials, is an ideal method to fabricate these materials.^{6–8} In recent years, different biotemplating routes have been developed for the conversion of biological materials into biomorphous SiO₂ ceramics. Shin *et al.*⁹ reported the fabrication of hierarchical porous SiO₂ ceramics from wood by a surfactant-templated

* Corresponding author. E-mails: zhongli-91@163.com; stjhfut@163.com
doi: 10.2298/JSC090410010Z



sol-gel process. Davis *et al.*¹⁰ produced ordered mesoporous silica by infiltration of bacteria with an SiO₂ gel. Cook *et al.*¹¹ exactly replicated butterfly structures by chemical vapor deposition of silica. However, for the application of bio-templates, how to control the pores shape and size distribution is still a challenge.

Wood is a biodegradable, recyclable, abundant and natural composite with cellulose, hemicellulose, and lignin as the major biopolymeric constituents with additional macromolecular compounds, such as different kinds of fat, oil, wax, resin, *etc.*, as minor constituents. Wood tissues are composed of interconnected cells (tracheids) and open spaces (lumens). These cells are glued together by an intercellular layer and are connected by openings of different shapes. These openings are called pits (bordered pits or simple pits) and are the communication channels between the cells.^{9,12} Owing to its stable and hierarchically porous characteristics, wood is an excellent template for porous structures.

In the present study, porous SiO₂ ceramics were fabricated using fir flour as the biological template structure. Fir wood (classified as coniferous) is composed of a unique cross-sectional constructed tracheid cells and bordered pits along the tracheid walls for tangential connectivity. Fir wood exhibits a nearly bimodal pore distribution. The scales range from mm *via* μm to nm.¹² However, the fine structure of the cellulose materials in fir wood is composed of crystalline and amorphous regions. The amorphous regions easily absorb chemicals, whereas the compactness of the crystalline regions makes it difficult for chemical penetration. To increase the pore volume and the corresponding possible amount of the infiltrated SiO₂ precursor, the fir flour was pretreated with a NaOH solution. The sol-gel infiltration process of a low viscous oxide precursor into the fir flour was applied. During burn out of the biological preforms during the calcination process, porous SiO₂ ceramics were obtained, which maintained the morphology of the fir flour. The microstructure, crystallinity change and chemical functional groups of fir flour and porous SiO₂ ceramics were investigated using field emission scanning electron microscopy (FESEM), X-ray diffraction (XRD) analysis and Fourier transform infrared (FTIR) spectroscopy.

EXPERIMENTAL

Material preparation

Fir wood (*Cunninghamia lanceolata*) was ground into flour of approximately 200 μm and dried at 105 °C for 24 h. Dried flour (2.5 g) was treated with 20 wt. % NaOH solution (100 mL) at 30 °C for 2 h in order to remove the fats and fatty acids in the flour. The NaOH-treated flour, which possessed a better connectivity and cellular affinity for the penetration of the precursor solution, was subsequently washed with distilled water until the wash water was alkali-free and then dried at 105 °C for 24 h. The precursor solution was prepared using tetraethyl orthosilicate (TEOS), ethanol (EtOH), distilled water and hydrochloric acid (HCl) in the molar ratio 1:4:4:0.05.

The NaOH-treated flour specimens were infiltrated with the precursor solution at 60 °C for 24 h in a self-made sealed infiltration vessel. Subsequently, the specimens were removed

from the precursor solution and dried in air at 130 °C for 24 h to form *in situ* SiO₂ gels. Finally, the infiltrated specimens were calcined by heating at a rate of 10° C/min to 600, 800 or 1000 °C and held at the desired temperature for 3 h to remove the template by oxidation and then allowed to cool to room temperature.

Characterization

A Fourier transformation, infrared spectrometer (Perkin–Elmer Spectrum 100) operating in the transmission mode under a dry air atmosphere was employed to record the FTIR spectra of the samples in the wavenumber range 4000–400 cm⁻¹ using the KBr pellet technique.

For crystalline phase identification, the X-ray diffraction patterns of the samples were measured on a powder X-ray diffraction meter (Rigaku D/Max-rB). The crystallinity index (I_c) was determined by using Eq. (1):

$$I_c = \frac{I_{(002)} - I_{(am)}}{I_{(002)}} \quad (1)$$

where $I_{(002)}$ is the counter reading at peak maximum at a 2θ angle close to 22°, representing crystalline material, and $I_{(am)}$ is the counter reading at peak maximum at a 2θ angle close to 18°, representing amorphous material in the cellulosic fir flour.

Field emission scanning electron microscopy (FEI Sirion 200, operated at 5 kV) was employed to observe the morphological features of the samples. For field emission scanning electron microscopy (FESEM) observations, the sample was pre-sputtered with a conducting layer of Au for 2 min at 10 kV.

The N₂ adsorption isotherms were measured with a Micromeritics ASAP 2020 adsorption analyzer. The pore size distributions (PSD) were calculated from the adsorption branches of the N₂ isotherms using the Barrett–Joyner–Halenda (BJH) method.

RESULTS AND DISCUSSION

FTIR Analysis

The spectra of fir flour, NaOH-treated flour, SiO₂ gel-treated flour composite and SiO₂ ceramics are shown in Fig. 1. In the spectra of the fir flour and NaOH-treated flour (Fig. 1, a and b, respectively), the absorption bands at 2928 and 1374 cm⁻¹ are attributed to the C–H stretching and bending vibration in cellulose. The absorption band of the C–O stretch vibrations in cellulose and hemicelluloses are at 1054 cm⁻¹, which is the highest intensity band. Furthermore, the vibration peak at 1732 cm⁻¹, attributed to the C=O stretching of methyl ester and carboxylic acid, were absent in the spectrum of the NaOH-treated flour. This indicated the removal of pectin, waxy and natural oils covering the external surface of the cell wall by the alkali treatment. The ratio of peak heights at 1374 and 2928 cm⁻¹ (H_{1374}/H_{2928}) in the FTIR spectra of the flour samples was used for the determination of the crystallinity index of cellulose in fir flour.¹³ In this study, the H_{1374}/H_{2928} ratio decreased from 1.2 for fir flour to 0.93 for the NaOH-treated flour, suggesting that the proportion of the amorphous material had increased in the NaOH-treated flour.

In the spectra of the SiO₂-gel/treated flour composite and SiO₂ ceramics calcined at 800 °C (Fig. 1, c and d, respectively), the absorption bands at 1090, 800

and 460 cm^{-1} are ascribed to the asymmetric and symmetric stretching vibrations of Si–O–Si bonds. In the FTIR absorption spectrum of the SiO_2 gel-treated flour composite (Fig. 1, c), peaks characteristic for both flour and SiO_2 absorption spectra appear, suggesting that no chemical reaction between the SiO_2 gel and the fir flour occurred during the infiltration. In the FTIR spectrum of the product obtained at a calcination temperature of $800\text{ }^\circ\text{C}$, the peaks assigned to fir flour became negligible and nearly only the peaks ascribed to the Si–O–Si asymmetric and symmetric stretching vibrations were evident, suggesting that the calcination went nearly to completion.

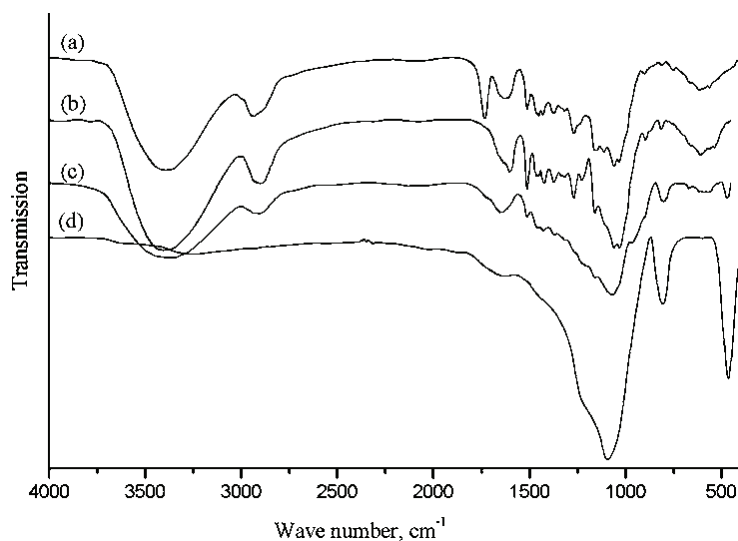


Fig. 1. FTIR Spectra of a) fir flour, b) NaOH-treated flour, c) SiO_2 gel-treated flour composite and d) SiO_2 ceramics calcined at $800\text{ }^\circ\text{C}$.

XRD Analysis

The XRD patterns of the fir flour, NaOH-treated flour, SiO_2 gel-treated flour composite and the SiO_2 gel dried at $110\text{ }^\circ\text{C}$ are shown in Fig. 2. The major diffraction planes of the cellulose in fir flour, namely the (101), (002) and (040) planes, are present at 2θ angles of 16.5 , 22.3 and 34.3° .¹⁴ The characteristic peak of cellulose can be seen in Fig. 2 (a and b). There was no crystalline transformation of the crystalline structure in the NaOH-treated flour. However, the NaOH treatment decreased the intensity of the (020) plane, suggesting that the degree of crystallinity of cellulose was decreased. The crystallinity index (I_c) decreased from 68 % for fir flour to 58 % for the NaOH-treated fir flour, suggesting that alkali treatment increased the proportion of amorphous material present in the fir flour as also suggested by FTIR results. In Fig. 2 (d), a broad peak centered at $2\theta = 23.2^\circ$ indicates that the SiO_2 gel was in the amorphous

state.¹⁵ Characteristic peaks of both fir flour and SiO₂ gel can be found in Fig. 2 (c). The broad peak at $2\theta = 23^\circ$ is formed by the overlapping the cellulose characteristic peak centered at $2\theta = 22.3^\circ$ and a SiO₂ gel relevant peak. The peak characteristic for cellulose at 16.5° has a lower intensity than that shown in Fig. 2 (b). The peak characteristic for cellulose at 34.3° was absent.

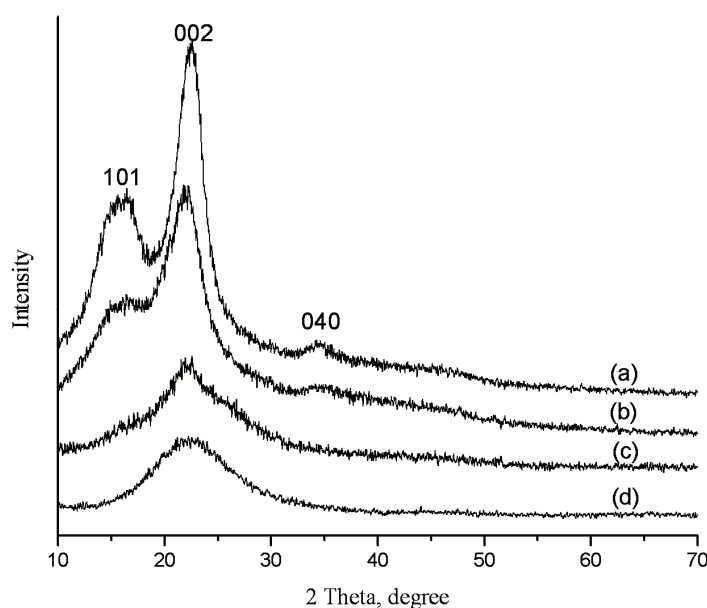


Fig. 2. XRD Patterns of a) fir flour, b) NaOH-treated flour, c) SiO₂ gel-treated flour composite and d) SiO₂ gel.

The XRD patterns of the SiO₂ ceramics calcined at 600, 800 and 1000 °C in air are illustrated in Fig. 3. According to these patterns, the original components of fir flour were completely removed. There is only one broad peak centered at $2\theta = 23.2^\circ$, suggesting that amorphous SiO₂ was formed during calcination at 600 and 800 °C in air. When the calcination temperature was increased to 1000 °C, the peak became somewhat sharper and more intense. The SiO₂ after calcination at 1000 °C in air had a typical cristobalite structure. There were eight crystal peaks at 2θ values of 21.8, 28.5, 31.1, 36.0, 42.5, 44.6, 46.8, and 48.5°, which correspond to (110), (111), (102), (200), (211), (202), (113) and (212). The calculated size of the SiO₂ using the Scherrer Equation was in the range 1.8–4.1 nm. Some amount of the tridymite structure was found as evidenced by the additional peaks at 2θ values of 20.8 and 27.5°.

FESEM Analysis

The SEM micrographs of fir flour, NaOH-treated flour, the SiO₂ gel-treated flour composite and the SiO₂ ceramics calcined at 800 °C are shown in Fig. 4.

The fir wood, which is a softwood, is composed of a unique cross-sectional constructed tracheid cell and bordered pits along the tracheid walls. Figs. 4a and 4b show that bordered pits of 5–10 μm can be observed on the cell walls, which are channels that connect the different tracheid cells and enhance their connectivity. By comparing Fig. 4b with Fig. 4d, it is evident that NaOH treatment can clean the surface of the flour, and enlarge the size of the pit pores. The highly uniform parallel tubular cellular structures and ordered arrays of bordered pits can be clearly observed (Fig. 4c). The pit pores at the tracheid walls are 10–15 μm in diameter (Fig. 4d).

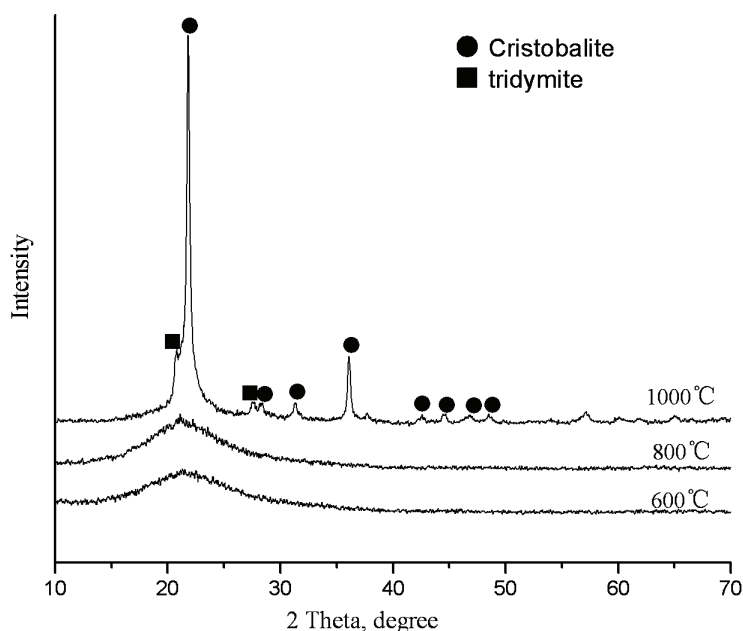


Fig. 3. XRD Patterns of NaOH-treated flour specimens infiltrated with SiO_2 ceramics calcined at various temperatures in air.

After the NaOH-treated fir flour had been infiltrated with SiO_2 sol, subsequent gelling and drying occurred, and an SiO_2 gel-treated flour composite was formed (Figs. 4e and 4f). It can be seen that the gel covered the surface of the flour and filled almost all the pores of tracheids and pits, suggesting that the SiO_2 sol penetrated the cell wall structures and condensed around the cellular tissues.¹⁶ Figures 4g and 4h show the SiO_2 ceramics calcined at 800 $^\circ\text{C}$. In comparison with the fir flour, the obtained ceramic materials retained the ordered pores structure of the fir flour. The array of tubular tracheid and pit pores were retained. However, the pit pores shrank to 1–5 μm , and some cracks on the walls were created by the thermal contraction.

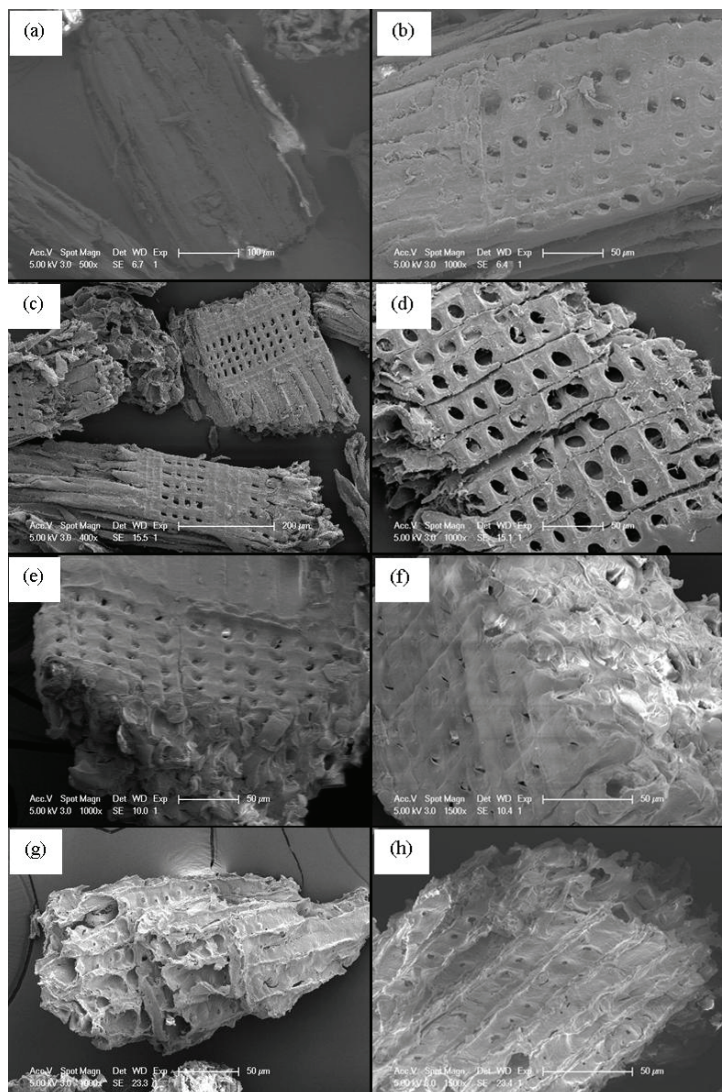
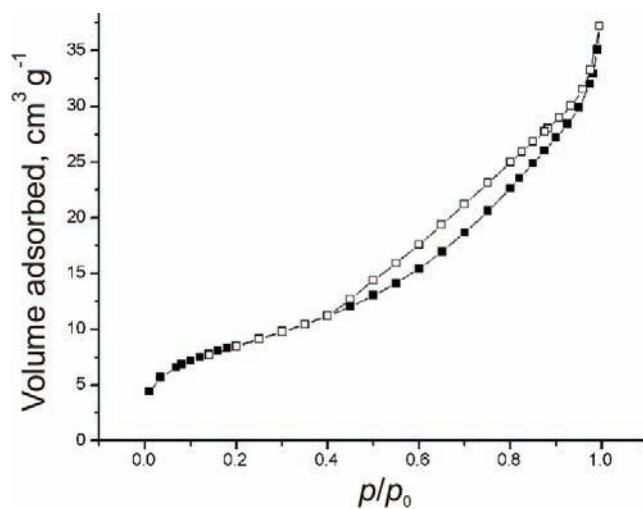


Fig. 4. SEM Micrographs of fir flour (a and b), NaOH-treated flour (c and d), SiO₂ gel-treated flour composite (e and f) and SiO₂ ceramics calcined at 800 °C (g and h).

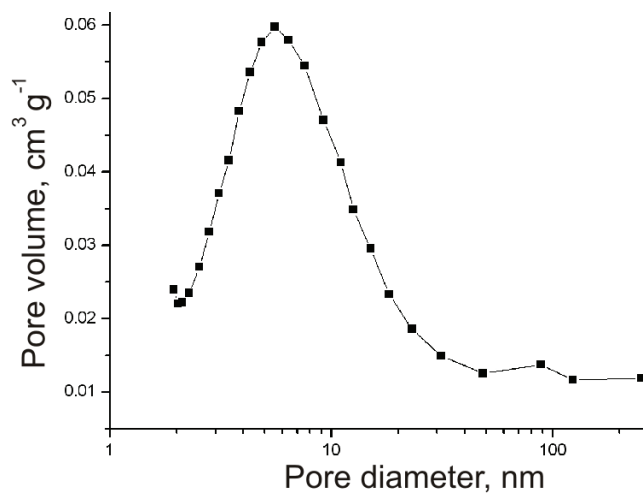
N₂ Adsorption measurement

From the N₂ adsorption measurement, the isotherms and corresponding PSD curves for SiO₂ ceramics calcined at 800 °C are shown in Figs. 5a and 5b, respectively. The obtained isotherm can be classified as type-IV according to the IUPAC classification with an H3 hysteresis loop. According to the PSD curves, the size distribution fell in the range of mesopore (2–40 nm), as can be seen in

Fig. 5b. The adsorption–desorption hysteresis occurs in the p/p_0 range 0.41–0.99, demonstrating that the materials contained mesopores of relatively uniform pore size. The H3 hysteresis loop indicates the asymmetric slot shape of the mesopores or channels coincidence with the tubular characteristics of the pores of the fir flour. Meanwhile, a narrow hysteresis loop illustrates an interconnected mesoporous system and high pore connectivity according to the percolation theory.¹²



(a)



(b)

Fig. 5. N_2 adsorption results of SiO_2 ceramics calcined at 800 °C, a) isotherm plots and b) PSD curves.

CONCLUSIONS

The structure of fir flour treated with 20 % NaOH solution was analyzed by FTIR spectroscopy, X-ray diffraction analysis and FESEM. The results show that most of the non-cellulosic components, such as pectin, waxy substances and natural oils, covering the external surface of the cell walls were removed and that the crystallinity of the fir flour was decreased after treatment, which changed the topography of the flour and increased the proportion of amorphous material present in the fir flour. The NaOH treatment was useful to achieve a net shape conversion of the complex structures and to increase the pore volume and the corresponding possible amount of the infiltrated precursor.

Porous SiO₂ ceramics were successfully prepared by a simple biotemplated process, *i.e.*, the infiltration of NaOH-treated fir flour with a low viscosity SiO₂ sol and subsequent heat treatment in air. The final oxide products retained the ordered pores structure and also exhibited unique pore size and distribution with a hierarchy on the nanoscale derived from the fir flour.

Acknowledgements. This work was supported by the National Science Foundation of China (No. 50773017).

ИЗВОД

МОРФОЛОГИЈА SiO₂ ДОБИЈЕНОГ ИЗ ШАБЛОНА ОД ПИЉЕВИНЕ ЈЕЛЕZHONG LI^{1,2}, TIEJUN SHI¹ и LIYING GUO¹

¹*School of Chemical Engineering, Hefei University of Technology, Hefei 23009* и ²*School of Chemical Engineering, Anhui University of Science & Technology, Huainan 232001, China*

Испитивано је добијање SiO₂ са контролисаном порозном структуром из шаблона од пиљевине јеле сол–гел поступком. Пиљевина јеле одређене крупноће, која је третирана 20 % раствором NaOH, филтрирана је SiO₂ солом мале вискозности и затим термички третирана у ваздуху, чиме се формира високопорозна структура SiO₂. Микроструктура SiO₂ и формирање фаза током поступка испитивани су дифракцијом X-зрака (XRD), инфрацрвеном спектроскопијом са Фуриеовим трансформацијама (FTIR) и скенирајућом електронском микроскопијом исијавања из поља (FESEM). Расподела пора по величини у коначном производу мерена је адсорпцијом N₂ (PSD). Резултати указују на то да се мења топографија површине и повећава удео аморфне фазе у пиљевини третираној раствором NaOH. Коначни оксидни производ задржао је уређену структуру пора и показао је униформну расподелу пора по величини, са хијерархијом на нано-нивоу добијеном из пиљевине јеле.

(Примљено 10. априла, ревидирано 25. новембра 2009)

REFERENCES

1. O. D. Velev, T. A. Jede, R. F. Lobo, A. M. Lenhoff, *Nature* **389** (1997) 447
2. B. T. Holland, C. F. Blanford, T. Do, A. Stein, *Chem. Mater.* **11** (1999) 795
3. O. D. Velev, E. W. Kaler, *Adv. Mater.* **12** (2000) 531
4. M. Kanungo, M. M. Collinson, *Chem. Commun.* **5** (2004) 548
5. M. E. Davis, *Nature* **417** (2002) 813

6. J. Cao, O. Rusina, H. Sieber, *Ceram. Int.* **30** (2004) 1971
7. Z. Liu, T. Fan, W. Zhang, D. Zhang, *Micropor. Mesopor. Mater.* **85** (2005) 82
8. A. Egelja, J. Gulicovski, A. Devecerski, B. Babić, M. Miljković, S. Bošković, B. Matović, *J. Serb. Chem. Soc.* **73** (2008) 745
9. Y. Shin, J. Liu, J. H. Chang, Z. Nie, G. J. Exarhos, *Adv. Mater.* **13** (2001) 728
10. S. A. Davis, S. L. Burkett, N. H. Mendelson, S. Mann, *Nature* **385** (1997) 420
11. G. Cook, P. L. Timms, C. G. Spickermann, *Ang. Chem. Int. Ed.* **42** (2003) 557
12. X. Li, T. Fan, Z. Liu, J. Ding, Q. Guo, D. Zhang, *J. Eur. Ceram. Soc.* **26** (2006) 3657
13. S. Y. Oh, D. I. Yoo, Y. Shin, H. C. Kim, H. Y. Kim, Y. S. Chung, W. H. Park, J. H. Youk, *Carbohydr. Res.* **340** (2005) 2376
14. L. Y. Mwaikambo, M. P. Ansell, *J. Appl. Polym. Sci.* **84** (2002) 2222
15. J. Locs, L. Berzina-Cimdina, A. Zhurinsh, D. Loca, *J. Eur. Ceram. Soc.* **29** (2009) 1513
16. Y. Shin, C. Wang, W. D. Samuels, G. J. Exarhos, *Mater. Lett.* **61** (2007) 2814.